Techno-environmental Simulations for Solar Energy-Powered Seawater Reverse Osmosis Desalination for a Hyper Arid Coastal Region

Sara Aldei*, Khawla Alshayji**, and Esra Aleisa***

**Renewable Energy Department, Energy and Building Research Center, Kuwait Institute for Scientific Research.*

***Chemical Engineering Department, College of Petroleum and Engineering, Kuwait University, P.O. Box 5969, Safat 13060, Kuwait.*

****The Industrial and Management Systems Engineering Department, College of Petroleum and Engineering, Kuwait University, P.O. Box 5969, Safat 13060, Kuwait.*

**** Corresponding Author: e.aleisa@ku.edu.kw*

Submitted : 08-06-2022

Revised : 16-09-2022

Accepted : 21-09-2022

ABSTRACT

This study investigates the efficiency of a solar-powered seawater desalination plant (DP) using reverse osmosis for an arid coastal region. The solar models are investigated using local meteorological data, including direct, diffused and global irradiance. The meteorological data are obtained using local typical meteorological data set collected from a ground weather station. The PVsyst simulation tool is used to model a grid-connected solar PV system utilizing three photovoltaic (PV) technologies: thin-film, monocrystalline, and polycrystalline. Three scenarios were considered: restricted area, daily water production and design capacity. The optimum configuration for the restricted area scenario at the seawater DP location considered is an on-grid thin-film module (170 W) with a tilt angle of 20° and an inverter unit of 2000 kW. The solution module area is 15,248 m2. The annual electricity production will be approximately 4251.1 MWh/y, which represents only 3.1% of the DP demand. Thin-films produce higher annual electricity than monocrystalline and polycrystalline silicon by 8.3% and 5.9%, respectively, but require 15.9% and 5.7% more space than monocrystalline and polycrystalline silicon, respectively. For Shuwaikh DP, a 30 MIGD DP will require a PV system with a capacity of 120 MWp at 30° tilt angles and 60 inverters. The design environmental impact was assessed using life cycle assessment (LCA). The carbon footprint will decrease from 7.3 x10-5 to 1.8 x10-5 (kg CO2 equivalent), for the 30 MIGD production. The fossil fuel depletion will decrease by approximately 80%. However, the large number of solar panels and the significant total ground area required for the 30 MIGD. The solar array of 1,531,054 m2 will adversely affect the urban land occupation impact category by 84% and will increase metal depletion by 37%. The response surface optimization indicates that the optimal performance in the coastal region for power desalination plants is achieved when using a thin-film at a tilt angle of 20 o.

Keywords: Photovoltaic (PV); Reverse Osmosis (RO), Desalination; Meteorological Data; Kuwait; Multicriteria optimization; Life cycle assessment (LCA).

Nomenclature

A	Total ground area required for PV panels
ALO	Agricultural land occupation
C	Clearance between PV panels
CC	Climate Change
CSP	Concentrated solar power
DNI	Direct normal irradiance
DHI	Diffused horizontal irradiance
DP	Desalination plant
FD	Fossil depletion
GHI	Global horizontal irradiance
GCR	Ground coverage ratio
HT	Human toxicity
KDWQI	Drinking water quality index
KDWQS	National drinking water quality standards
KISR	Kuwait Institute for Scientific Research
LCA	Life cycle assessment
MD	Metal depletion
MED	Multi-effect distillation
MEW	Ministry of electricity
MEWRE	Ministry of electricity and water and renewable energy
MIGD	Million imperial gallons per day
MSF	Multi-stage flash distillation
MT	Metal depletion
NLT	Natural land transformation
PMF	Particulate matter formation
PV	Photovoltaic
R	Active ground area
RE	Renewable Energy
RO	Reverse Osmosis
RSI	Rotating shadow-band irradiometer
S	Space between PV panels
SDG	Sustainable development goal
Si-Mono	Monocrystalline-silicon
Si-Poly	Polycrystalline-silicon
STC	Standard test condition
SWRO	Seawater Reverse Osmosis
τ	PV tilt angle
TAC	Terrestrial acidification
TMY	Typical meteorological year
UAE	United Arab Emirates
ULO	Urban land occupation

1- INTRODUCTION

Nonconventional water resources such as desalination are the backbone for water provision in Kuwait and most hyper-arid regions. Kuwait scores high on the sustainable development goal (SDG) indicator 6.1: to achieve universal and equitable access to safe and affordable drinking water before 2030 (Sachs et al., 2021), as this has been a national target for Kuwait since 1979 as per the water decree 7/1/1979. Kuwait has consistently scored 'outstanding' on the Drinking Water Quality Index (KDWQI), issued by the National Drinking Water Quality Standards (KDWQS) (MEW, 2019). This outstanding achievement, despite its unarguable importance, carries a hefty price tag, mainly due to the extensive energy requirements of seawater desalination (Al-Shayji & Aleisa, 2018; Aleisa & Al-Shayji, 2018; Aljuwaisseri et al., 2022). Electricity and water desalination cogeneration have been shown to adversely contribute to many environmental impact categories, including climate change (CC), human toxicity (HT), marine equitoxicity, terrestrial ecotoxicity, abiotic depletion, acidification, ozone depletion, and photochemical oxidation, among others (Al-Shayji & Aleisa, 2018; Aleisa & Heijungs, 2020). Kuwait's national vision 'New Kuwait 2035' (SCPD, 2019) calls for remedial action in the country's sectors to combat CC, which includes shifting to renewables. In particular, by 2030, Kuwait is aiming to have 15% of its energy mix from renewable sources. As a result, the name and strategy of the Kuwait Ministry of Electricity (MEW) was changed to the Ministry of Electricity and Water and Renewable Energy (MEWRE) in March 2021. To date, the implementation toward the renewable transition has been modest (Alsayegh, 2021).

Research to address the efficiency of renewable energy (RE) for the dual water and energy challenge has been increasingly significantly, according to the literature (Mito et al., 2019). Photovoltaic (PV) reverse osmosis (RO) membrane desalination systems or PV-RO account for more than one-third of the installed capacity for renewable powered desalination, followed by wind-driven RO (12%), solar membrane desalination (11%), solar multi-effect distillation (MED) (9%), solar MED and dehumidification (9%) and solar multi-stage flash distillation (MSF) (7%) (Gude & Fthenakis, 2020).

The majority of solar desalination systems decouple electricity and water production and support decentralization (Azinheira et al., 2019; Gude & Fthenakis, 2020). Examples of RO-PV systems include the Australian landmark project Perth Seawater RO (SWRO) desalination plant (DP). This DP is powered by a wind farm north of Perth. The plant is designed to optimize the energy consumption and requires 3.4 kWh/m^3, including overhead, and 2.2 kWh/m^3 for the plant only (ESTAP IRENA, 2012). Masdar Institute in the United Arab Emirates (UAE) inaugurated a renewable energy desalination program in 2015 (Masdar, 2020). It tested SWRO desalination technologies that consumed less than 3.6 kWh per cubic meter of desalinated water. At the Al-Hamriyah SWRO DP in Sharjah, UAE, the daily electrical power demand is 281.24 MWh is satisfied by a hybrid system of RE that is complemented by power generated from the grid (Ghenai et al., 2018). This system is economically feasible with a high renewable fraction of 47.3%, low excess power of 0.15%, low levelized cost of energy of $90/MWh, and low CO_2 emissions of 264.25 kg/MWh. The AlKhafji SWRO at King Abdulaziz City for Science and Technology is PV powered (10 MW). It generates 60 K -90 K m^3/day of desalinated water (KSA Vision, 2019). Recent research shows that the share of desalination using RE is only approximately 1% (ALJ, 2018). Technological advancement together with political and socioeconomic factors have influenced its progress (Alsayegh, 2021).

The objective of this study is to simulate different RO-PV seawater desalination configurations for the meteorological conditions of Kuwait. The simulations compile configurations of different PV technologies, tilt angles, and areas required for the PV array to power production. The assessment is conducted across different scenarios that constrain the space, demand and capacity and accordingly estimates the monthly electrical power production based on local meteorological data. The results are further optimized using multicriteria response surface optimization. The environmental assessment is conducted using life cycle assessment (LCA) in accordance with ISO 14040/4 (ISO 14040, 2020). The results have wider repercussions toward promoting SDGs, 6: clean water, 7: affordable and clean energy, and 13: for climate action.

2- LITERATURE REVIEW

Solar desalination systems are classified into direct and indirect systems and thermal or nonthermal systems (Ali et al., 2011). Baig et al. (2018) integrated PV with heat exchangers connected to an RO plant to enhance the overall system efficiency. Their results indicate raised panel temperature, which resulted in a counter performance, that was addressed by cooling the PV panels. Mannot et al. (2018) used simulation to configure PV-RO plants for the highest performance while minimizing cost. Technoeconomic analysis was also conducted by Gökçek (2018), a hybrid RO system that uses wind turbines and PV. The electricity cost for that system is $0.308/kWh, which results in a desalination cost of $2.20/$m^3$. Osman et al. (2016) analyzed a pilot plant of a Fresnel solar collector system combined with a thermal desalination plant in Saudi Arabia. The results showed that the breakeven of fuel cost in which the levelized cost of water was equal for the two cases studied was $92/bbl, while the total yearly direct normal irradiance (DNI) on the site was 1132 kWh/m^2. The fuel break-even cost fell to $52/bbl when the integrated solar desalination system was run at a location with a relatively high total annual DNI (1937 kWh/m^2). The study indicated that combining a Fresnel Solar Collection system with MED was more cost efficient when operated without thermal energy storage. Cioccolanti and Renzi (2018) studied the potential of coupling heliostat concentrated solar power (CSP) with a single effect seawater thermal desalination. Iaquaniello, Mari, Salladini, Mabrouk, and Fath (2014) analyzed a hybrid power desalination scheme in which MED was powered by the low temperature exhaust steam delivered from the back pressure steam turbine, while the electricity produced by the turbine was used to power the RO. Sajjad and Rasul (2015) developed a computational model to simulate the performance of a small-scale solar desalination system using Aspen Plus process simulation software. Bataineh (2016) integrated a thermos-compressor MED driven by solar power to desalinate 50K m^3/day in Aqaba, Jordan.

3- COUNTRY CONTEXT

Kuwait has eleven DPs (MEW, 2020), three of which operate using RO (Shuwaikh and Al-Zour South, and Doha West), one operates using MED (Al-Zour North), and the remaining DPs operate using MSF (cogeneration) (Al-Shayji & Aleisa, 2018; Aleisa & Al-Shayji, 2018; Aleisa & Heijungs, 2020). RO comprises 12% of the total water production using desalination in Kuwait (Aljuwaisseri et al., 2022). Reliable resource and characterization assessments are the first steps for the successful design of an RE project. Kuwait Institute for Scientific Research (KISR) has conducted a solar resource assessment based on both ground-based observations and satellite-based modeling. KISR has installed five

ground radiometric stations throughout Kuwait: Sabriyia, Alshagaya, Mutribah, Um Gudair, and Kabd, equipped with a thermopile pyranometer to measure the global horizontal irradiance (GHI) and a rotating shadow-band irradiometer (RSI) to measure the GHI, diffused horizontal irradiance (DHI), DNI and other weather variables. The solar irradiance and weather data are recorded in 10-minute and hourly time increments (AL-Rasheedi et al., 2014). Figure 1 shows the long-term average annual sum of (a) GHI and (b) DNI in Kuwait calculated by the SOLARGIS (2019) model from atmospheric and satellite data. The GHI is the most important parameter used for energy yield calculations and performance assessments of flat-plate PV technology. DNI is more relevant to the performance of CSP and concentrator solar PV technologies.

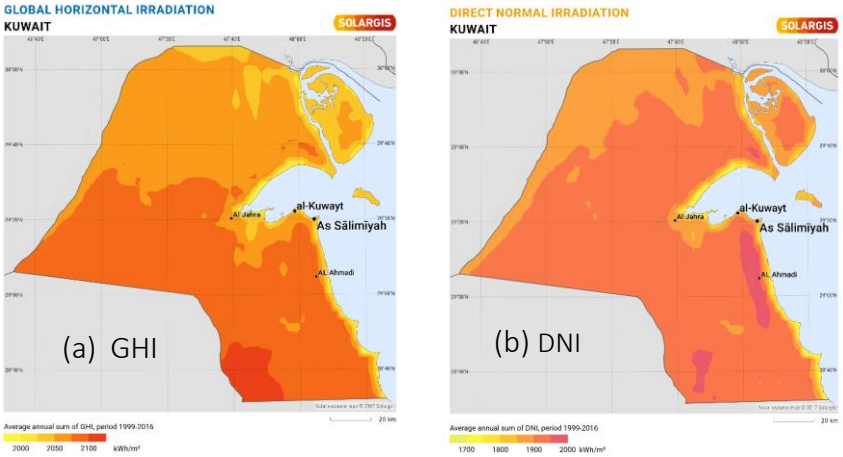

Figure 1: Solar resource map of Kuwait by SolarGIS (2019): (a) GHI and (b) DNI.

4- METHODOLOGY

The study framework provided in Figure 2 investigates three main PV technologies: thin-film, monocrystalline-silicon (Si-Mono), and polycrystalline-silicon (Si-Poly). The power output of the PV system is investigated based on the solar radiation intensity and the PV cell operating temperature for three tilt angles (τ): 20°, 25° and 30°. The meteorological data collected include the temperature, humidity, DNI, DHI and wind speed. DNI is the direct solar radiation beam that reaches the Earth's surface directly from the sun. DHI is the solar radiation that is reflected or scattered by ground or atmospheric particles, such as clouds, dust, or other particles (Alasfour et al., 2020; Bessa et al., 2021). The area required for the PV array is calculated for each simulation by changing the tilt angle of the PV modules to compare the ground coverage ratio (GCR) and the land area required for the PV array. PVsyst software simulates a grid-connected solar PV system using three technologies for three scenarios: constraining the available PV panel area, annual electricity consumption based on current production, and design based on full capacity. The applied configurations comprise an on-grid, ground-based free-standing structure with PV modules mounted at a fixed position to minimize battery use. Excessive power during the peak season or during plant maintenance is supplied to the utility grid.

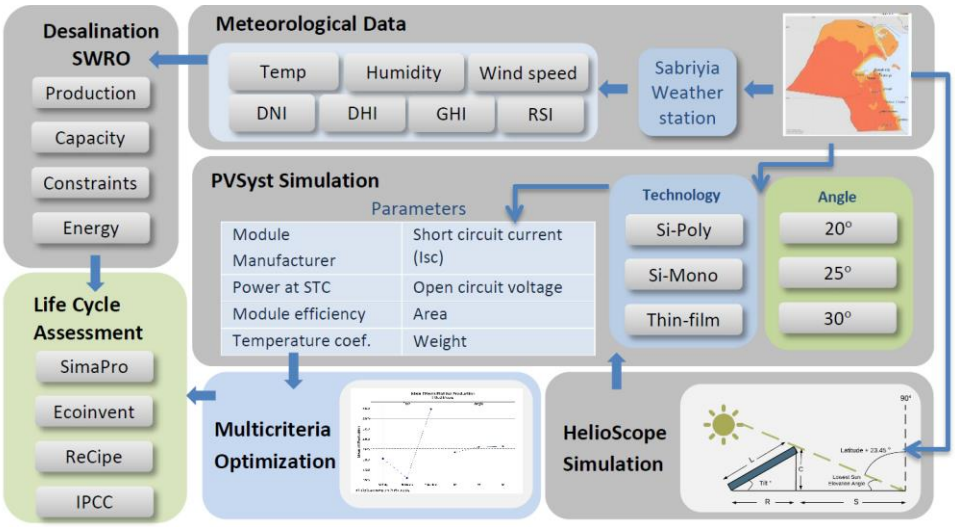

Figure 2: PV-RO simulation methodology.

Nine simulations using PVsyst are modeled to design a grid-connected solar PV system with a fixed capacity of 2000 kWp. The ohmic loss value is set to 1.5%, the power loss at the maximum power point due to mismatching is 1%, and the soiling loss is 3%. Due to humidity, the soiling loss is also considered. Table 1 shows the parameters of the PV modules used in the simulation.

Table 1: Parameters of PV Modules.

Technology	***Si-Poly***	***Si-Mono***	***Thin-Film***
Power at STC*	285 W	285 W	170 W
Module efficiency	14.78%	16.45%	13.9%
Temperature coefficient	-0.43%/°C 4.2 mA/°C	-0.39%/°C 4.9 mA/°C	-0.31%/°C 0.2 mA/°C
Short circuit current (Isc)	8.370 A	9.730 A	2.2 A
Open circuit voltage (Voc)	44.90 V	39.20 V	112 V
Area (Length, width, thickness)	1.940 m^2 (1956 mm, 992 mm, 50 mm)	1.731 m^2 (1016 mm, 1704 mm, 36 mm)	1.228 m^2 (1257 mm, 977 mm, 35 mm)
Weight	27 kg	19 kg	20 kg

*STC: Standard Test Condition (25 °C, 1000 W/m^2, 1.5 air mass).

The area calculated includes the shading effect factor. Larger shading by modules occurs when the sun elevation angle is low during winter, reaching 37.18° for Kuwait. The total GCR for any tilt angle is calculated using the ratio of active area (the area that is occupied with PV modules) to the total ground area (which is the active area plus the spacing between PV rows) (Figure 3). Let τ be the tilt angle; then, the active ground area (R), is calculated using $\alpha\cos(\tau)$, and the clearance (C), is calculated using $R = \alpha\sin(\tau)$. The spacing (S), between the PV rows is calculated using $C/\tan(\min\tau)$. The total ground area (A), is the summation of R and S. Finally, the GCR is calculated using R/A.

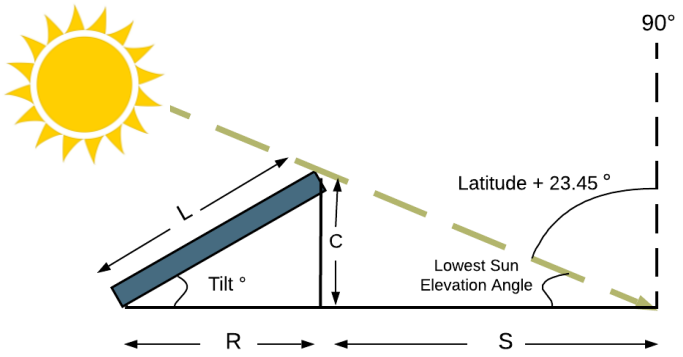

Figure 3: GCR calculation of the space required.

The HelioScope simulation tool is used to assess the site and design a solar PV system in accordance with the requirements of an existing Shuwaikh SWRO DP for a total capacity of 30 million imperial gallons per day (MIGD) (Aljuwaisseri et al., 2022). The HelioScope design parameters are supplied to PVsyst to simulate the annual energy output and the percentage of the total electricity production to supply the desalination (see Appendix A). The meteorological data are obtained from the ground weather station at Sabriya, which is also closest to the coastal areas at which the DP is located (AL-Rasheedi et al., 2014). An hourly typical meteorological year (TMY) dataset is compiled and averaged from the data collected over three years (2013-2015) from ground weather stations to be used in PVsyst; data include temperature, wind speed, relative humidity, DNI, and DHI. The results of the PVsyst are fed to a multicriteria response surface optimizer that solves for the best angle and technology to maximize renewable energy output while minimizing space. The optimization is conducted using Minitab v.21.1. Finally, the result is assessed environmentally using LCA in ISO 14040/4 (ISO 14040, 2020) using the Ecoinvent inventory database and the Recipe and IPCC impact assessment methods.

5- RESULTS

Nine simulation models were compiled for three solar energy technologies using three tilt angles over three scenarios (constraints). The annual energy production and *A* are provided in

Table **2**. The resulting GCR is 0.6743, 0.6177, and 0.5662 for the three angles of 20°, 25°, and 30°, respectively.

Table 2: Results for the PV-RO simulations using HelioScope.

No.	Technology	τ°	Plant Capacity (kWp)	Number of Modules	Module Area (m^2)	Energy production (MWh/y)	*A* (m^2)
1	Si-Poly	20	2001	7020	13621	3786	20200.2
2		25				3813	22051.1
3		30				3816	24056.8
4	Si-Mono	20	2000	7018	12150	3692	18018.6
5		25				3718	19669.7
6		30				3721	21458.8
7	Thin-film	20	2000	11766	14450	4028	21429.6
8		25				4055	23393.2
9		30				4056	25521.0

The results indicate that a τ of 30° achieved the highest annual electricity production in Kuwait. The results also indicate that reducing the tilt angle of the PV module from 30° to 25° reduces the energy output by approximately 0.08% for Si-Poly and Si-Mono and 0.02% for the thin-film. A τ of 20° reduces the output by 0.78% for both Si-Poly and Si-Mono and 0.69% for the thin-film. In terms of space, reducing the τ to 25° saves the space of the PV array by 8.3%. A τ

of 20° reduces the ground area required by 16%. The thin-film using a τ of 30° produced a higher annual energy output than Si-Poly and Si-Mono by 8.3% and 5.9%, respectively. However, the thin-film required additional spaces of 15.9% and 5.7% compared to Si-Mono and Si-Poly, respectively, for the same capacity.

5.1 Scenario 1: Constrained Space Area for PV panels

The simulation using the HelioScope tool indicates that the maximum capacity able to be installed at Shuwaikh DP's location is 2110 kWp (see Figure 4). While constraining the capacity, the optimum configuration is an on-grid thin-film module (170 W) with a τ of 20° and an inverter unit of 2000 kW. The solution module area is 15,248 m^2. The annual electricity production will be approximately 4251.1 MWh/y, which represents only 3.1% of the average annual electrical consumption required for the Shuwaikh SWRO DP and 1.7% of the electricity demand for full capacity. Figure 5 shows the potential monthly electricity production for the first scenario. Using a τ of 20°, the GCR equals 0.6743, and the total ground area required for the PV system equals 22,613 m^2. Figure 4 shows a satellite image of the Shuwaikh SWRO DP with a solar PV system using thin-film PV modules with a 20° tilt angle to maximize the energy output for the constrained space scenario, which was generated using the HelioScope tool.

Figure 4: Satellite image of the Shuwaikh DP with the PV modules using HelioScope simulation.

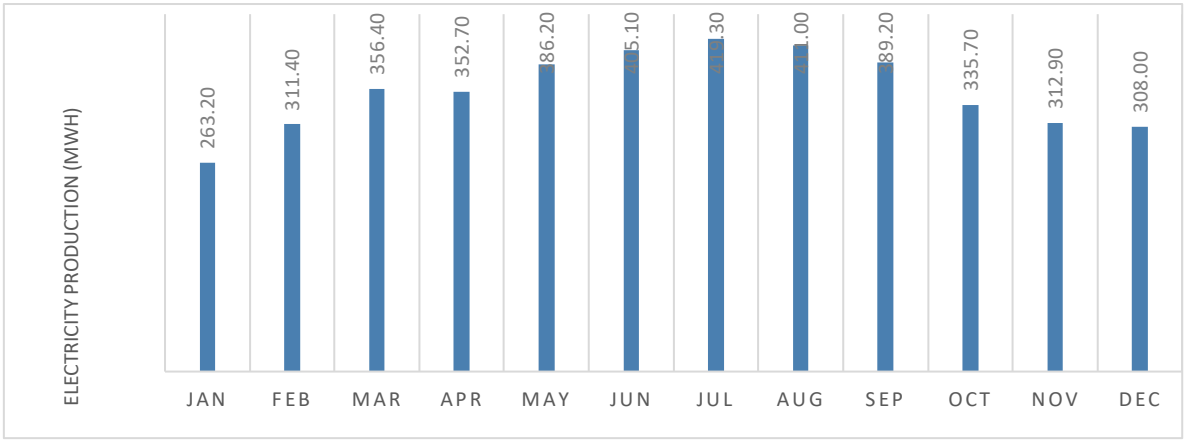

Figure 5: Expected monthly electricity production using the first scenario: Space restriction.

5.2 Scenario 2: Constrained Annual Electrical Demand

In this scenario, the panels could be installed in a nearby open area with similar meteorological conditions. The system was constrained to the total annual electrical needs of the Shuwaikh SWRO DP based on its current operation. The best simulation produced 70 MWp using thin-film modules with a 30° tilt angle. This system will require 35 units of 2 MW rated power inverters, a module area of 505,688 m^2, and a total ground area of 893,126 m^2 with GCR equal to 0.5662. This system will produce 15 MIGD.

5.3 Scenario 3: Maximum Capacity of Electrical Demand

In this scenario, all nine simulations were compiled to achieve SWRO plants operating at a maximum design capacity of 30 MIGD. This system will require 120 MWp from thin-film PV modules τ of 30° using 60 inverters. The area needed for the modules is 866,883 m^2, and the total ground area required for the solar array is 1,531,054 m^2 with GCR equal to 0.552. this shows that for Kuwait, desalinating 1 MIGD of seawater to potable quality using RO requires 51035.13 m^2 land area of solar panels. For the current production of 455.5 MIGD, if SWRO was used, it will require a total land space of 23.3 km^2.

5.4 Multicriteria Optimization

Multicriteria response surface optimization is applied to maximize electricity output and minimize the A required for the solar panels. The main effect plots and optimization results are provided in Figure 6 and in Figure 7, respectively. For the coastal location in Kuwait, the optimal solution is a thin-film with a τ of 20°. The composite response surface desirability index is 0.7 with a 95% confidence intervals of (21405.6, 21449.6) for A (m^2) and (4025.75, 4030.81) for energy output (MWh/y).

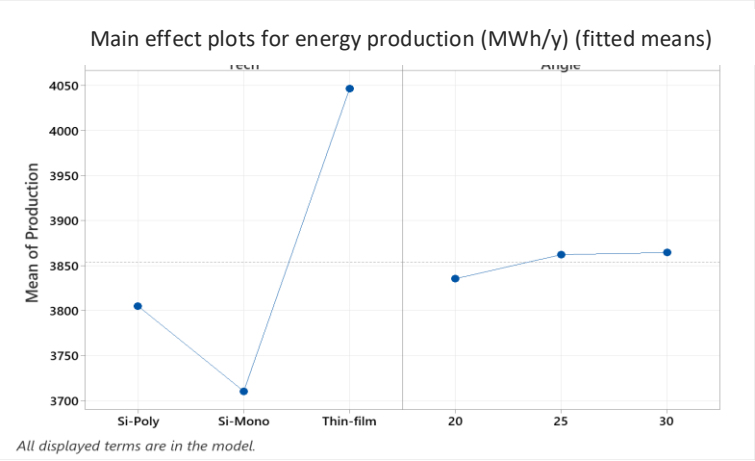

Figure 6: Main effects plots using Minitab (v.21.1).

Parameters

Response	Goal
A (m2)	Minimum
Production (MWh/y)	Maximum

Solution

Solution	Angle	Tech	A (m2) Fit	Production (MWh/y) Fit	Composite Desirability
1	20	Thin-film	21427.6	4028.28	0.709969

Multiple Response Prediction

Variable	Setting
Angle	20
Tech	Thin-film

Response	Fit	SE Fit	95% CI	95% PI
A (m2)	21427.6	5.1	(21405.6, 21449.6)	(21395.6, 21459.7)
Production (MWh/y)	4028.28	0.59	(4025.75, 4030.81)	(4024.59, 4031.97)

Figure 7: Response surface optimization results using Minitab (v.21.1).

5.5 Environmental Impact

The environmental impact is determined using LCA in accordance with ISO 14040/4 (ISO 14040, 2020). The goal is to compare the use of PV panels versus natural gas to operate the Shuwaikh SWDP. The functional unit is 30 MIGD of desalinated water. The system boundary is gate-to-gate. The detailed inventories for PV can be obtained from (Aljuwaisseri et al., 2022) and for natural gas from (Aleisa & Heijungs, 2020); additional data on membrane inventories can be found in (Aleisa et al., 2022). The life cycle impact assessment results using the Recipe V1.10 midpoint (H) method are provided in Figure 8 (a). The carbon footprint using the IPCC 2013 method (Stocker et al., 2014) is provided in Figure 8 (b). Additional midpoint characterization and normalized analysis are provided in Appendix B. The results indicate that using solar energy will reduce CC by 75%, fossil depletion (FD) by 80% and particulate matter formation (PMF) by 63%. However, the downside is the vast total ground area required for the solar array, which is equal to 1,531,054 m^2 with a ground coverage ratio of 0.552. Hence, PV panels increase urban land occupation (ULO) by 84% due to the substantial land requirements for solar panels. The metal depletion (MD) rate also increases by 37% due to the metals and materials required for the panels. The kg CO_2 equivalent decreases from 7.3 $x10^{-5}$ to 1.8 $x10^{-5}$ using the IPCC 2013 method (see Figure 8 (b)).

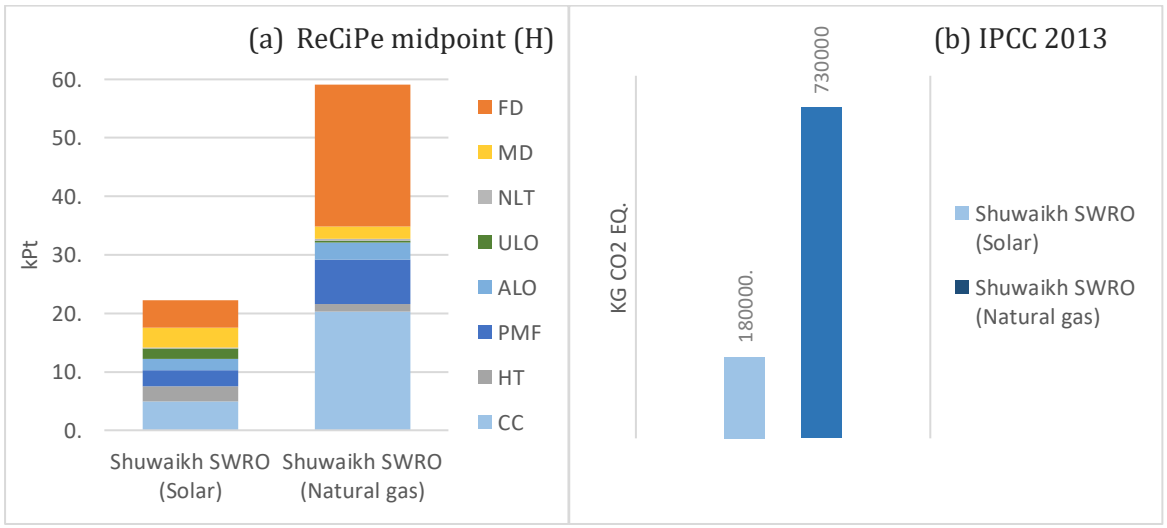

Figure 8: Single score results for comparing Shuwaikh SWDP using solar energy versus natural gas compared for 30 MIGD using (a) ReCipe midpoint (2016) and (b) IPCC (2013). CC: Climate change, HT: Human toxicity, PMF: Particulate matter formation, ALO: Agricultural land occupation, ULO: Urban land occupation, NLT: Natural land transformation, MT: Metal depletion, FD: Fossil depletion.

6 CONCLUSIONS

This study publishes the analysis of techno-environmental grid-connected solar PV system parameters to power SWRO desalination plants in Kuwait. The simulation is based on three-year hourly meteorological data collected from the Sabriya ground weather station, which is located near the coastline. The long-term average annual sum of the GHI, DNI DHI, ambient temperature, humidity and wind speed were collected on hourly basis and averaged over a three year period. Three PV technologies, thin-film, Si-Mono, and Si-Poly, were investigated across three tilt angles: 20°, 25° and 30°. The HelioScope simulation tool was used to assess the site and design a solar PV system in accordance with the requirements of an existing Shuwaikh SWRO DP for a total capacity of 30 MIGD. The HelioScope design parameters were supplied to PVsyst to simulate the annual energy output. Accordingly, the percentage of the total electricity production supplied to the DP is calculated. The analysis indicates that the maximum power capacity of the PV system that can be fitted in the area available in the Shuwaikh SWRO desalination plant is 2110 kWp. However, this capacity can only satisfy 3.1%, as it can modestly produce 930K IG per day. The required output of the PV system to power the current daily water production rate at Shuwaikh DP demands 70 MWp, which will occupy a considerable 505,688 m^2 panel space. Operating the Shuwaikh SWRO on design capacity requires 120 MWp with a 1,531,054 m^2 ground area for the PV system. The analysis shows that the optimum title angle for the PV modules in terms of annual energy production in Kuwait is 30°. However, decreasing the tilt angle of the modules from 30° to 20° decreases the annual energy output from the same capacity of PV systems by 0.78% for Si-Poly and Si-Mono and 0.69% for thin-film. Decreasing the tilt angle of the module to 20° improves the energy production during the summer season. Although thin-film PV modules are expected to produce lower efficiency than Si-Poly and Si-Mono in general, when using regional coastal data and local relatively low temperature coefficients, the multicriteria response surface optimization indicates the optimal setting of a tilt angle of 30° and thin-film for Kuwait coastal areas. The environmental impact of the solar panels was assessed using LCA. The results indicate that using solar energy will reduce the CC by 75%, FD by 80% and PMF by 63%. However, the downside is the vast total ground area required for the solar array, which increases ULO by 84%. It also increases MD by 37%. The kg CO_2 equivalent decreases from 7.3 $x10^{-5}$ to 1.8 $x10^{-5}$. Future research needs to be directed toward investigating hybrid energy mixes coupled with hybrid desalination technologies through the implementation of a thorough techno-economic assessment that considers regional meteorological conditions.

ACKNOWLEDGMENTS

The authors acknowledge the valuable assistance of Dr. Majed Al-Rasheedi from the Kuwait Institute for Scientific Research.

APPENDIX A

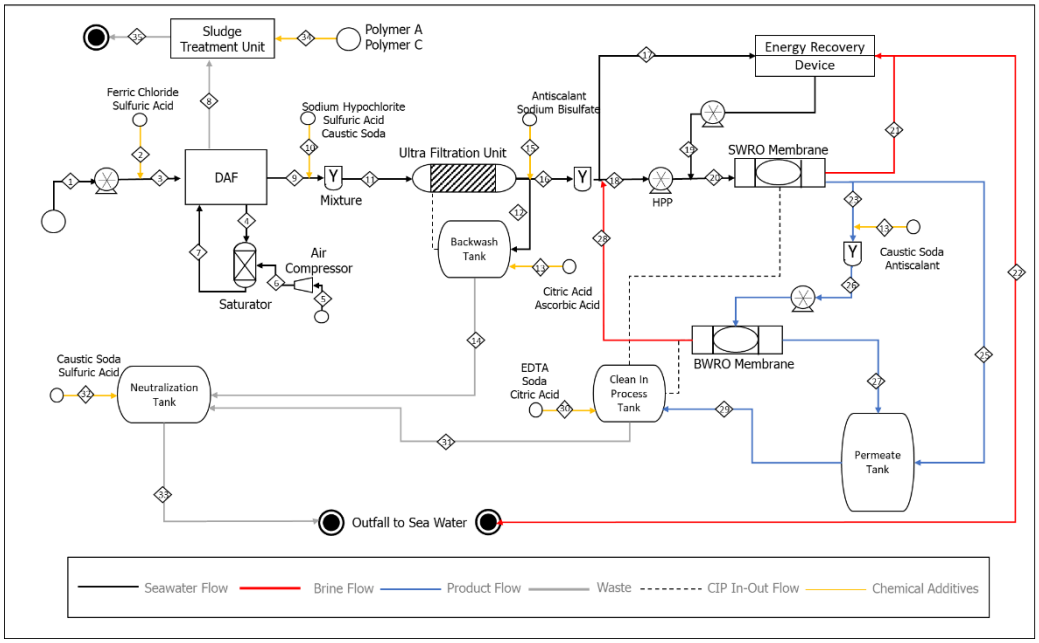

Figure A.1: AlShuwaikh SWRO DP (Aljuwaisseri, Aleisa, & Alshayji, 2022).

Table A.1. Parameters of the Inverters Used in the analysis

Inverter Manufacturer	----
Nominal AC power	2000 kW
Nominal maximum power voltage (Vmpp)	450 V
Minimum voltage (Vmin)	450 V
Maximum voltage (Vmax)	750 V
Maximum efficiency	98.2 %

Table A.2. Parameters of (Si-Poly) Module.

Module Manufacturer	Generic (Si-poly)
Power at STC*	285 W
Module efficiency	14.78 %
Temperature coefficient	-0.43 %/°C 4.2 mA/°C
Short circuit current (Isc)	8.370 A
Open circuit voltage (Voc)	44.90 V
Area (Length, width, thickness)	1.940 m^2 (1956 mm, 992 mm, 50 mm)
Weight	27 kg

*STC: Standard Test Condition (25°C, 1000 W/m^2, 1.5 air mass).

Table A.3. Parameters of Mono-Crystalline Silicon Module.

Module Manufacturer	Si-mono
Power at STC	285 W
Module efficiency	16.45 %
Temperature coefficient	-0.39 %/°C 4.9 mA/°C
Short circuit current (Isc)	9.730 A
Open circuit voltage (Voc)	39.20 V
Area (Length, width, thickness)	1.731 m^2 (1016 mm, 1704 mm, 36 mm)

Weight	19 kg

Table A.4. Parameters of Thin-Film Module.

Module Manufacturer	Thin-film
Power at STC	170 W
Module efficiency	13.9 %
Temperature coefficient	-0.31 %/°C 0.2 mA/°C
Short circuit current (Isc)	2.2 A
Open circuit voltage (Voc)	112 V
Area (Length, width, thickness)	1.228 m^2 (1257 mm, 977 mm, 35 mm)
Weight	20 kg

APPENDIX B

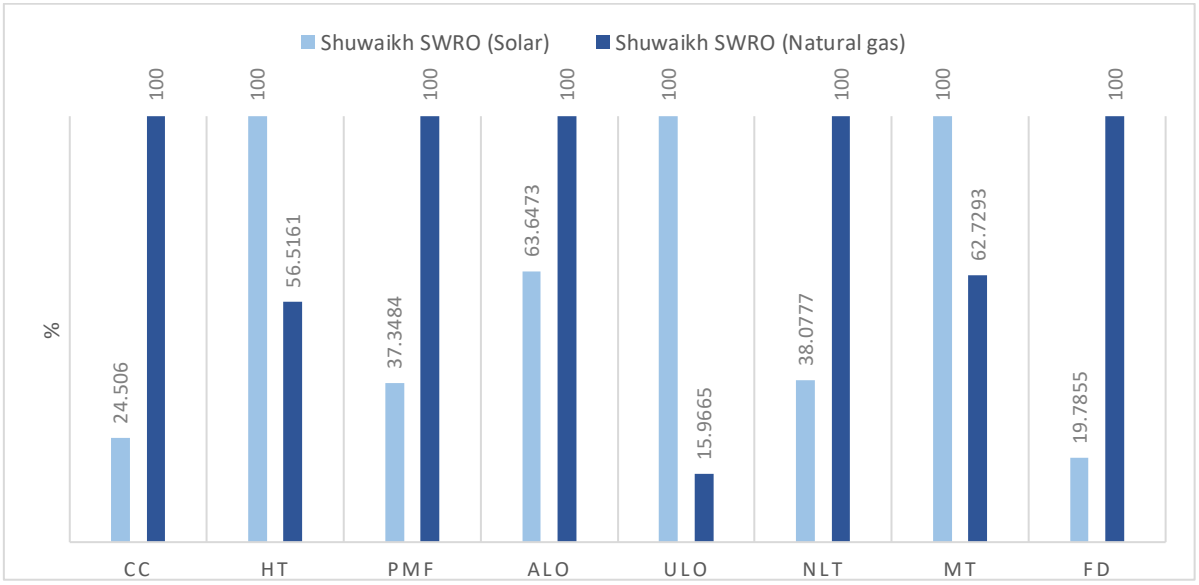

Figure B.1: Characterized results for comparing Shuwaikh SWDP using solar energy versus natural gas

compared using the ReCiPe midpoint (H) v1.10 for 30 MIGD. CC: Climate change, HT: Human toxicity, PMF: Particulate matter formation, ALO: Agricultural land occupation, ULO: Urban land occupation, NLT: Natural land transformation, MT: Metal depletion, FD: Fossil depletion.

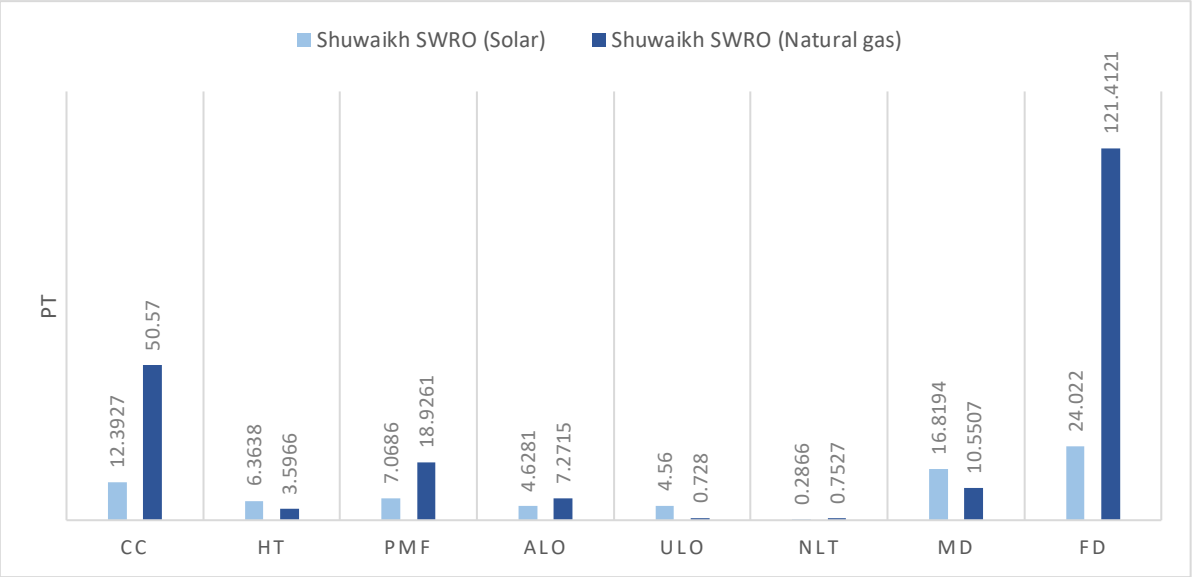

Figure B.2: Normalized results for comparing Shuwaikh SWDP using solar energy versus natural gas compared using the ReCiPe midpoint (H) v1.10 for 30 MIGD. CC: Climate change, HT: Human toxicity, PMF: Particulate matter formation, ALO: Agricultural land occupation, ULO: Urban land occupation, NLT: Natural land transformation, MT: Metal depletion, FD: Fossil depletion. Measured in points (pt) which is a composite normalized index used in the ReCiPe midpoint method.

REFERENCES

AL-Rasheedi, M., Gueymard, C., Ismail, A., & AL-Hajraf, S. 2014. Solar resource assessment over kuwait: Validation of satelite-derived data and reanalysis modeling. EuroSun, Aix-Les-Bains, France.

Al-Shayji, K., & Aleisa, E. 2018. Characterizing the fossil fuel impacts in water desalination plants in kuwait: A life cycle assessment approach. Energy, 158 681-692. https://doi.org/https://doi.org/10.1016/j.energy.2018.06.077

Alasfour, A., Alkandary, A. R., & Alzubi, F. G. 2020. Device and method for measuring effect of soiling on photovoltaic device. In: Google Patents.

Aleisa, E., Al-Mutairi, A., & Hamoda, M. 2022. Reconciling water circularity through reverse osmosis for wastewater treatment for a hyper-arid climate: A life cycle assessment. Sustainable Water Resources Management, 883-99. https://doi.org/10.1007/s40899-022-00671-8

Aleisa, E., & Al-Shayji, K. 2018. Ecological–economic modeling to optimize a desalination policy: Case study of an arid rentier state. Desalination, 43064-73. https://doi.org/doi.org/10.1016/j.desal.2017.12.049

Aleisa, E., & Heijungs, R. 2020. Leveraging life cycle assessment and simplex lattice design in optimizing fossil fuel blends for sustainable desalination. The International Journal of Life Cycle Assessment, 25(4):744-759. https://doi.org/10.1007/s11367-020-01738-4

Ali, M., Fath, H., & Armstrong, P. 2011. A comprehensive techno-economical review of indirect solar desalination. Renewable and Sustainable Energy Reviews4187- 4199.

ALJ. 2018. Saudi arabia: Ready to lead the world in smart city development? Abdul Latif Jameel Periodical.

Aljuwaisseri, A., Aleisa, E., & Alshayji, K. 2022. Environmental and economic analysis for desalinating seawater of high salinity using reverse osmosis: A life cycle assessment approach. Environment, Development and Sustainability. https://doi.org/10.1007/s10668-022-02214-9

Alsayegh, O. A. 2021. Barriers facing the transition toward sustainable energy system in kuwait. Energy Strategy Reviews, 38100779. https://doi.org/https://doi.org/10.1016/j.esr.2021.100779

Azinheira, G., Segurado, R., & Costa, M. 2019. Is renewable energy-powered desalination a viable solution for water stressed regions? A case study in algarve, portugal. Energies, 12(24):4651. https://www.mdpi.com/1996-1073/12/24/4651

Baig, H., Jani, R., Markam, B. K., Maiti, S., & Mallick, T. K. 2018. Modelling and experimental analysis of a seasonally tracked v-trough pv/t in india. Solar Energy, 170618-632.

Bataineh, K. 2016. Multi-effect desalination plant combined with thermal compressor driven by steam generated by solar energy. Desalination39-52.

Bessa, J. G., Micheli, L., Almonacid, F., & Fernández, E. F. 2021. Monitoring photovoltaic soiling: Assessment, challenges, and perspectives of current and potential strategies. iScience, 24(3):102165. https://doi.org/https://doi.org/10.1016/j.isci.2021.102165

Cioccolanti, L., & Renzi, M. 2018. Coupling a small-scale concentrated solar power plant with a single effect thermal desalination system: Analysis of the performance. Applied Thermal Engineering1046--1056.

ESTAP IRENA. 2012. Water desalination using renewable energy: Technology brief. www.etsap.org – www.irena.org

Ghenai, C., Merabet, A., Salameh, T., & Pigem, E. C. 2018. Grid-tied and stand-alone hybrid solar power system for desalination plant. Desalination, 435172-180.

Gökçek, M. 2018. Integration of hybrid power (wind-photovoltaic-diesel-battery) and seawater reverse osmosis systems for small-scale desalination applications. Desalination, 435210-220.

Gude, V. G., & Fthenakis, V. 2020. Energy efficiency and renewable energy utilization in desalination systems. Progress in Energy, 2(2):022003. https://doi.org/10.1088/2516-1083/ab7bf6

Iaquaniello, G., Salladini, A., Mari, A., Mabrouk, A. A., & Fath, H. E. S. 2014. Concentrating solar power (csp) system integrated with med--ro hybrid desalination. Desalination121-128.

ISO 14040. 2020. Environmental management. Life cycle assessment.Requirements and guidelines. Amendment 2. In. Geneva: The International Organization for Standardization (ISO).

KSA Vision.2019. Water desalination project using solar power. Saudi Vision 2030. https://www.vision2030.gov.sa/v2030/v2030-projects/water-desalination-project-using-solar-power/

Masdar. 2020. Renewable energy water desalination programme. https://masdar.ae/

MEW. 2019. Kuwait drinking water quality index (Water resources and develpment center, Issue.

MEW. 2020. Statistical year book 2020 (water). M. o. E. Water. https://www.mew.gov.kw/media/ovad3xpl/2019-كتاب-المياه.pdf

Mito, M. T., Ma, X., Albuflasa, H., & Davies, P. A. 2019. Reverse osmosis (ro) membrane desalination driven by wind and solar photovoltaic (pv) energy: State of the art and challenges for large-scale implementation. Renewable and Sustainable Energy Reviews, 112669-685. https://doi.org/https://doi.org/10.1016/j.rser.2019.06.008

Monnot, M., Carvajal, G. D. M., Laborie, S., Cabassud, C., & Lebrun, R. 2018. Integrated approach in eco-design strategy for small ro desalination plants powered by photovoltaic energy. Desalination, 435246-258.

Osman, O., Kosaka, H., Bamardouf, K., Al-Shail, K., & Al-Ghamdi, A. 2016. Concentrating solar power for seawater thermal desalination. Desalination70-78.

Sachs, J. D., Kroll, C., Lafortune, G., Fuller, G., & Woelm, F. 2021. Sustainable development report 2021: The decade of action for the sustainable development goals. Cambridge University. https://doi.org/10.1017/9781009106559

Sajjad, M., & Rasul, M. 2015. Simulation and optimization of solar desalination plant using aspen plus simulation software. Procedia Engineering739-750.

SCPD. 2019. Kuwait voluntary national review 2019.

SOLARGIS.2019. Retrieved Dec 18 from solargis.com

Stocker, T. F., Qin, D., Plattner, G.-K., Tignor, M. M., Allen, S. K., Boschung, J., Nauels, A., Xia, Y., Bex, V., & Midgley, P. M. 2014. Climate change 2013: The physical science basis. Contribution of working group i to the fifth assessment report of ipcc the intergovernmental panel on climate change.